

# Voids fill us in on rising cosmology tensions

Sofia Contarini  <sup>1,2,3</sup> Alice Pisani  <sup>4,5,6</sup> Nico Hamaus  <sup>7</sup> Federico Marulli <sup>1,2,3</sup>  Lauro Moscardini <sup>1,2,3</sup>  and Marco Baldi <sup>1,2,3</sup> 

<sup>1</sup>Dipartimento di Fisica e Astronomia “Augusto Righi” - Alma Mater Studiorum Università di Bologna, via Piero Gobetti 93/2, I-40129 Bologna, Italy

<sup>2</sup>INFN-Sezione di Bologna, Viale Berti Pichat 6/2, I-40127 Bologna, Italy

<sup>3</sup>INAF-Osservatorio di Astrofisica e Scienza dello Spazio di Bologna, Via Piero Gobetti 93/3, I-40129 Bologna, Italy

<sup>4</sup>Center for Computational Astrophysics, Flatiron Institute, 162 5th Avenue, 10010, New York, NY, USA

<sup>5</sup>The Cooper Union for the Advancement of Science and Art, 41 Cooper Square, New York, NY 10003, USA

<sup>6</sup>Department of Astrophysical Sciences, Peyton Hall, Princeton University, 4 Ivy Lane, Princeton, NJ 08544, USA

<sup>7</sup>Universitäts-Sternwarte München, Fakultät für Physik, Ludwig-Maximilians-Universität, Scheinerstrasse 1, 81679 München, Germany

## Abstract

We investigate the main tensions within the current standard model of cosmology from the perspective of the main statistics of cosmic voids, using the final BOSS DR12 data set. For this purpose, we present the first estimate of the  $S_8 \equiv \sigma_8 \sqrt{\Omega_m}/0.3$  and  $H_0$  parameters obtained from void number counts and shape distortions. To analyze void counts we rely on an extension of the popular volume-conserving model for the void size function, tailored to the application on data, including geometric and dynamic distortions. We calibrate the two nuisance parameters of this model with the official BOSS collaboration mock catalogs and propagate their uncertainty through the statistical analysis of the BOSS void number counts. The constraints from void shapes come from the study of the geometric distortions of the stacked void-galaxy cross-correlation function. In this *Letter* we focus our analysis on the  $\Omega_m$ - $\sigma_8$  and  $\Omega_m$ - $H_0$  parameter planes and derive the marginalized constraints  $S_8 = 0.813^{+0.093}_{-0.068}$  and  $H_0 = 67.3^{+10.0}_{-9.1} \text{ km s}^{-1} \text{ Mpc}^{-1}$ , which are fully compatible with constraints from the literature. These results are expected to notably improve in precision when analyzed jointly with independent probes and will open a new viewing angle on the rising cosmological tensions in the near future.

*Unified Astronomy Thesaurus concepts:* cosmology: observations, cosmological parameters, large-scale structure of universe, methods: statistical

## 1. Introduction

In recent years, anomalies in the observations of the Universe at large scales have puzzled the scientific community. These are expressed as statistically relevant discrepancies, or tensions, between the cosmological constraints obtained from late (i.e. low-redshift) and early (i.e. high-redshift) probes.

The most significant tension affects the estimate of the Hubble constant,  $H_0$ , describing the present expansion rate of the Universe. In particular, the so-called *Hubble tension* concerns the mismatch between the Planck collaboration results obtained from the cosmic microwave background (CMB) anisotropies (Planck Collaboration et al. 2020), and the direct local distance ladder measurements based on type Ia supernovae (SN Ia, Riess

et al. 2022). These two estimates are in disagreement by about  $5\sigma$  (see, e.g., Di Valentino et al. 2021a). Second in order of importance is the tension on the matter clustering strength, often quantified by the parameter  $S_8 \equiv \sigma_8 \sqrt{\Omega_m}/0.3$ , derived from the matter density parameter  $\Omega_m$  and the root mean square of density fluctuations on an  $8 \text{ h}^{-1} \text{Mpc}$  comoving scale,  $\sigma_8$ . In this case the discrepancy of the Planck satellite measurements relates to low-redshift probes, like weak gravitational lensing and galaxy clustering, with a statistical disagreement at the level of  $2\text{-}3\sigma$  (see, e.g., Di Valentino et al. 2021b).

These observational tensions may reveal the presence of systematic errors in the cosmological measurements or, alternatively, the requirement to modify the current benchmark  $\Lambda$ -cold dark matter ( $\Lambda$ CDM) model of cosmology. This has led to the proposal of a plethora of alternatives to the  $\Lambda$ CDM model, involving physics beyond the standard model of particle physics (see Abdalla

Corresponding author: Sofia Contarini  
 sofia.contarini3@unibo.it

et al. 2022, and references therein). Despite the fact that some of the proposed models alleviate one or more discrepancies (see, e.g., Pandey et al. 2020; Di Valentino et al. 2021c; Schöneberg et al. 2022), we are still longing for a definitive solution that provides a comprehensive and satisfactory description of all the cosmological observables.

In this context, the darkest regions of our Universe may supply a fundamental and independent contribution in shedding light on the rising cosmological tensions. These vast underdense zones, scarcely populated by galaxies and other luminous objects, are commonly referred to as *cosmic voids*. Within the last decade, voids have begun to assert their relevance as cosmological probes (Pisani et al. 2019; Moresco et al. 2022). Recent works have indeed exploited voids to test the standard cosmological model (e.g., Hamaus et al. 2016, 2020; Aubert et al. 2022; Nadathur et al. 2020; Woodfinden et al. 2022; Kovács et al. 2022) and others have provided promising forecasts on the constraining power expected from different void statistics with the upcoming redshift surveys, such as *Euclid* (Laureijs et al. 2011; Amendola et al. 2018; Hamaus et al. 2022; Contarini et al. 2022a; Bonici et al. 2022).

Nevertheless, up until now the void size function as a first-order statistic of voids has never been exploited to derive cosmological constraints. In this work we extend the results presented in Contarini et al. (2022b), where we performed a statistical analysis of the size distribution of voids identified in the final data release (DR12) of the Baryon Oscillation Spectroscopic Survey (BOSS, Eisenstein et al. 2011; Dawson et al. 2013). We focus on the main cosmological tensions and we add to our results the contribution from the constraints achieved by Hamaus et al. (2020), who relied on that same data to analyze void shape distortions. This combination allows us to provide a first estimate of the  $S_8$  and  $H_0$  parameters derived from cosmic voids. We discuss our results in the current context of cosmology, featuring the constraints from different surveys and cosmological probes.

This *Letter* is structured as follows. In Section 2 we present the theory of the void size function, together with the galaxy and void catalogs we employed. In Section 3 we describe the cosmological analysis performed in this work. The constraints obtained in this context are then presented in Section 4 and compared with other important results from the literature. Finally, in Section 5 we draw the conclusion of this work.

## 2. Theory and data sets

### 2.1. Void size function model

The void size function model predicts the comoving number density of voids as a function of their size. It was originally developed by Sheth & van de Weygaert (2004) on the basis of the excursion-set theory and at its core relies on the multiplicity function:

$$f_{\ln \sigma_R} = 2 \sum_{j=1}^{\infty} \exp \left( -\frac{(j\pi x)^2}{2} \right) j\pi x^2 \sin(j\pi \mathcal{D}), \quad (1)$$

with  $\mathcal{D} = \frac{|\delta_v^L|}{\delta_c^L + |\delta_v^L|}$  and  $x = \frac{\mathcal{D}}{|\delta_v^L|} \sigma_R$ ,

which describes the volume fraction of the Universe occupied by cosmic voids. In Equation (1) all the quantities are expressed in linear theory, as indicated by the superscript ‘‘L’’. In particular,  $\sigma_R$  is the root mean square variance of linear matter perturbations on a scale  $R_L$ , while  $\delta_c^L$  and  $\delta_v^L$  are the density contrasts required for the formation of dark matter halos and cosmic voids, respectively. Only the latter threshold significantly affects the predicted void size distribution at large scales and determines the linear density contrast embedded inside cosmic voids. We highlight the importance of this quantity further below, but refer the reader to Contarini et al. (2022b) for a more complete description.

To calculate the density of cosmic voids as a function of their radii  $R$  in the nonlinear regime, Jennings et al. (2013) proposed the following expression:

$$\frac{dn}{d \ln R} = \frac{f_{\ln \sigma_R}}{V(R)} \frac{d \ln \sigma_R^{-1}}{d \ln R_L} \Big|_{R_L=R_L(R)}, \quad (2)$$

which is called *volume-conserving model* (Vdn hereafter). As the name suggests, it relies on the conservation of the total volume  $V$ , occupied by voids in the transition from the linear to the nonlinear regime. The Vdn model has been tested successively in different works (see, e.g., Jennings et al. 2013; Ronconi et al. 2019; Verza et al. 2019; Contarini et al. 2021), but for its application to voids identified in a biased distribution of tracers (e.g., galaxies and clusters of galaxies) a modification of its main assumptions is required.

To take into account the change in the density contrast when voids are traced by biased objects, Contarini et al. (2019) introduced a simple parametrization of the underdensity threshold of the Vdn model. This strategy was then revisited in Contarini et al. (2022b) to take into account the degeneracy of the tracer effective bias with the normalization of the matter density fluctuations,  $\sigma_8$ , leading to the following parametrization of

the void density threshold:

$$\delta_{v,DM}^{\text{NL}} = \frac{\delta_{v,tr}^{\text{NL}}}{\mathcal{F}(b_{\text{eff}}, \sigma_8)}, \text{ with} \quad (3)$$

$$\mathcal{F}(b_{\text{eff}} \sigma_8) = C_{\text{slope}} b_{\text{eff}} \sigma_8 + C_{\text{offset}}.$$

In this equation, we use the subscript “NL” to highlight quantities computed in nonlinear theory. Furthermore,  $\delta_{v,tr}^{\text{NL}}$  is the density contrast used to define voids in the tracer density field (tr), while  $\delta_{v,DM}^{\text{NL}}$  is the corresponding value in the matter density field (DM, i.e. dark matter particles). The function  $\mathcal{F}(b_{\text{eff}} \sigma_8)$  parametrizes the action of the tracer effective bias  $b_{\text{eff}}$ , which depends on redshift and on the selected tracers (e.g., their host-halo mass).  $C_{\text{slope}}$  and  $C_{\text{offset}}$  are redshift-independent coefficients of the linear function  $\mathcal{F}$  and their dependence on the cosmological model can be considered negligible (Contarini et al. 2021). Moreover, Contarini et al. (2022a) demonstrated that the parametrization presented in Equation (3) is effective in encapsulating redshift-space distortions on cosmic voids, i.e. the enlargement of their observed radii caused by the peculiar motions of their tracers.

The presented extension of the Vdn model predicts the size function of voids identified by biased tracers in redshift space with good accuracy, provided the calibration of the nuisance parameters of the model,  $C_{\text{slope}}$  and  $C_{\text{offset}}$ , is performed via mock catalogs designed to reproduce the target tracer population (see Contarini et al. 2021, for further details). Hereafter, we will refer to this theoretical framework as the *extended Vdn* model.

## 2.2. Galaxy and void catalogs

In this work we analyze the BOSS DR12 data set (Reid et al. 2016), composed of the two target selections LOWZ and CMASS featuring more than one million galaxies with spectroscopic redshifts. We further use 100 realizations of the MultiDark PATCHY mocks (Kitaura et al. 2014, 2016; Klypin et al. 2016; Rodríguez-Torres et al. 2016), specifically designed to mimic the properties of the BOSS galaxies, to calibrate the nuisance parameters of the extended Vdn model (see Section 2.1).

Following the procedure of Contarini et al. (2022b), we divide the catalogs into two redshift bins, i.e.  $0.2 < z \leq 0.45$  and  $0.45 < z < 0.65$ , and measure  $b_{\text{eff}} \sigma_8$  for each case, as required in Equation (3). We estimate this quantity by modeling the multipoles of the galaxy two-point correlation function with the prescriptions of Taruya et al. (2010) (see Appendix A of Contarini et al. 2022b for further details). For the BOSS galaxies this yields  $b_{\text{eff}} \sigma_8 = 1.36 \pm 0.05$  in the interval  $0.2 < z \leq 0.45$  and  $b_{\text{eff}} \sigma_8 = 1.28 \pm 0.06$  in the  $0.45 < z < 0.65$  interval.

To identify cosmic voids in the distribution of real and mock galaxies we apply the public Void IDentification and Examination toolkit<sup>1</sup> (VIDE, Sutter et al. 2015), based on the code ZOnes Bordering On Voidness (ZOBOV, Neyrinck 2008). VIDE exploits the Voronoi tessellation technique to approximate a continuous density field and identifies its local minima. From this a catalog of voids is built by means of a watershed algorithm (Platen et al. 2007). We run VIDE on the entire galaxy distribution from the northern and southern Galactic hemispheres and assume the same cosmological model used to build the MultiDark PATCHY simulations to convert redshifts to comoving distances, i.e. a Planck2013 cosmology (Planck Collaboration et al. 2014, see also Section 3).

Once voids are identified, we process the extracted sample to match the theoretical definition used in the void size function model. In particular, we apply the cleaning procedure developed by Ronconi & Marulli (2017), publicly available in the *free software* C++/Python libraries CosmoBolognaLib<sup>2</sup> (Marulli et al. 2016), which rescales voids such that they exhibit a fixed density contrast of  $\delta_{v,tr}^{\text{NL}} = -0.7$ . This choice of under-density threshold is not unique, but is especially suited to obtain a statistically reliable void sample (see, e.g., Contarini et al. 2022a, for further details).

We then measure number counts of the cleaned voids as a function of their size. We first use the average PATCHY void number counts to calibrate the values of  $C_{\text{slope}}$  and  $C_{\text{offset}}$  through a Markov chain Monte Carlo (MCMC) analysis. The best-fit values we obtain for the coefficients of  $\mathcal{F}(b_{\text{eff}} \sigma_8)$  are  $C_{\text{slope}} = -1.62^{+0.66}_{-0.73}$  and  $C_{\text{offset}} = 4.30^{+0.94}_{-0.86}$ , but we refer the reader to Contarini et al. (2022b) for a complete presentation of these results. We then exploit the calibration performed with the PATCHY mocks to model the BOSS void number counts, sampling the posterior distribution of the free parameters of the extended Vdn model (see Section 3). We underline that the effectiveness of the analysis we apply in this work has been tested in Appendix B of Contarini et al. (2022b), where the methodology is thoroughly validated on PATCHY mocks.

## 3. Analysis

The cosmological analysis we carry out in this work is based on Bayesian inference. We take as data set the void counts extracted from the BOSS DR12 and assume a Poissonian likelihood (Sahlén et al. 2016). Our model is based on the extended Vdn theory, so it depends on

<sup>1</sup> [https://bitbucket.org/cosmicvoids/vide\\_public](https://bitbucket.org/cosmicvoids/vide_public)

<sup>2</sup> <https://gitlab.com/federicomarulli/CosmoBolognaLib>

the cosmological model and on the nuisance parameters  $C_{\text{slope}}$  and  $C_{\text{offset}}$  (see Section 2.1).

We consider a flat  $\Lambda$ CDM model with fiducial parameters given by Planck2013 results (Planck Collaboration et al. 2014) to be consistent with the ones used to build the MultiDark PATCHY simulations:  $\Omega_m = 0.307115$ ,  $H_0 = 67.77 \text{ km s}^{-1} \text{ Mpc}^{-1}$ ,  $\Omega_b = 0.048206$ ,  $n_s = 0.9611$  and  $\sigma_8 = 0.8288$ . Our statistical analysis is aimed at investigating the degeneracies in the  $\Omega_m - \sigma_8$  and  $\Omega_m - H_0$  planes, so we focus on two sets of cosmological parameters, the first characterized by wide uniform priors for  $\Omega_m$  and  $\sigma_8$ , and the second for  $\Omega_m$  and  $H_0$ . In both cases we marginalize over the remaining cosmological parameters by assigning to them uniform priors centered on our fiducial cosmology, with a total width of ten times the 68% uncertainties provided by Planck2018 constraints (Planck Collaboration et al. 2020). We also marginalize over  $C_{\text{slope}}$  and  $C_{\text{offset}}$  by considering their joint posterior distribution obtained from the calibration with PATCHY mocks.

We finally sample the posterior distribution of the considered parameter sets following an MCMC technique. At each step of the MCMC we consider a new set of cosmological parameters, compute the void size function and rescale the predicted void radii to model the effect of geometric distortions acting at the mean redshift of the selected void sample. The latter arise when assuming a wrong cosmology in the redshift-distance conversion, causing a distortion of the observed void shape along the directions parallel and perpendicular to the line of sight. The resulting anisotropy is referred to as Alcock-Paczynski (AP) effect (Alcock & Paczynski 1979) and can be modeled via two scaling parameters  $q_{\parallel}$  and  $q_{\perp}$  (e.g., Sánchez et al. 2017). Let us indicate with  $r_{\parallel}^*$  and  $r_{\perp}^*$  the observed comoving distances between two objects at redshift  $z$ , projected along the parallel and perpendicular line-of-sight directions, respectively. To obtain their corresponding length in the true cosmological model, we use:

$$\begin{aligned} r_{\parallel} &= \frac{H^*(z)}{H(z)} r_{\parallel}^* \equiv q_{\parallel} r_{\parallel}^*, \\ r_{\perp} &= \frac{D_A(z)}{D_A^*(z)} r_{\perp}^* \equiv q_{\perp} r_{\perp}^*. \end{aligned} \quad (4)$$

In these equations the starred quantities are computed assuming the fiducial cosmology.  $H(z)$  is the Hubble parameter and  $D_A(z)$  the comoving angular-diameter distance, which in flat  $\Lambda$ CDM are defined as:

$$\begin{aligned} H(z) &= H_0 [\Omega_m (1+z)^3 + 1 - \Omega_m]^{1/2} \quad \text{and} \\ D_A(z) &= \int_0^z \frac{c}{H(z')} dz', \end{aligned} \quad (5)$$

respectively. The inclusion of geometric distortions in the void size function model causes a shift in the predicted radius distribution that depends on the discrepancy between the true and the assumed fiducial cosmology. We finally underline that we did not account for super-sample covariance in our model, which recently has been demonstrated to only marginally affect the void size function (Bayer et al. 2022).

To gather additional cosmological information from cosmic voids, we present in Section 4.1 the constraints derived by adding to our analysis the contribution of the void-galaxy cross-correlation function measured in the same BOSS DR12 data set. Specifically, we rely on the findings of Hamaus et al. (2020): utilizing voids as standard spheres to measure geometric distortions, these authors constrained the growth rate of structure and provided a precise estimate of the total matter density parameter, i.e.  $\Omega_m = 0.312 \pm 0.020$ . We exploit this constraint by imposing a Gaussian prior on  $\Omega_m$  in the MCMC analysis. This approach is equivalent to multiplying the resulting posterior distributions from the two analyses, assuming these void statistics to be completely independent.

This assumption is supported by the results presented in Kreisch et al. (2022), where the cross-correlation between the void size function and the void-galaxy cross-correlation function is shown to be low. We also highlight that, conversely to what is presented in Kreisch et al. (2022), the sample of voids employed here for the study of number counts has undergone a cleaning procedure (see Section 2.2). This fact further reduces the correlation between the two void statistics, since the samples of voids considered in both works present different features.

## 4. Results

### 4.1. Cosmological constraints from cosmic voids

In this section we present the main results of the analysis, expressed as new cosmological constraints from the BOSS DR12 data set. These results supplement the constraints presented in Contarini et al. (2022b).

In Figure 1 we present the cosmological constraints from the void size function, in both the parameter planes analyzed, namely  $\Omega_m - \sigma_8$  and  $\Omega_m - H_0$ . As a reference, we also report the constraints obtained when omitting the AP effect in our model (see Section 3). This allows us to quantify the impact of the geometric distortion correction on voids and the subsequent small improvement on the cosmological constraints. We underline that this correction is generally negligible for collapsed and virialised structures, like galaxy clusters, because of their detachment from the Hubble expansion. We tested the

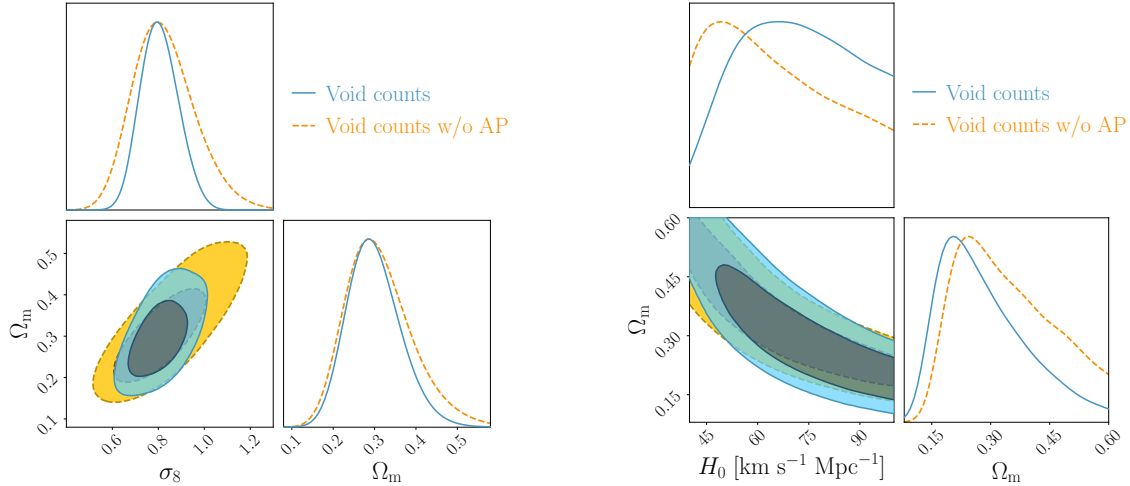


**Figure 1.** 68% and 95% confidence contours from void counts (in light blue) compared to the confidence contours obtained without including the void radius correction for the AP effect (in orange, see Section 3). We show on the left the cosmological constraints for the  $\Omega_m$ - $\sigma_8$  parameter plane, and on the right those for the  $\Omega_m$ - $H_0$  parameter plane.

effectiveness of the AP correction with PATCHY mocks, by assuming different fiducial values of  $\Omega_m$ , verifying that we recover the cosmological parameters of the simulation within 68% of the uncertainty.

We now compare our results with those obtained with other void statistics and cosmological probes, starting by focusing on the  $\Omega_m$ - $\sigma_8$  parameter plane. In the left panels of Figure 2 we report our constraints from void counts together with the estimate of  $\Omega_m$  from Hamaus et al. (2020) from void shape distortions, already introduced in Section 3 and reported here as a continuous band. In the same plot, we present the product of the posterior density probability of the two void statistics. With the contribution from void shape distortions, we obtain  $\Omega_m = 0.308^{+0.021}_{-0.018}$  and  $\sigma_8 = 0.809^{+0.072}_{-0.068}$ . In the right panels we compare this latter result with the confidence contours computed by Lesci et al. (2022) with the mass function of clusters identified in the third data release of the Kilo Degree Survey (KiDS-DR3) and those of the combined analysis of galaxy clustering and weak gravitational lensing<sup>3</sup> performed by the Dark Energy Survey Collaboration et al. (2018) with data from the first year of observations (DES Y1).

The joint analysis of different void statistics we present in this *Letter* is meant to show the full potential of voids as cosmological probes. However, we highlight that the most valuable gain is expected from the combination of the constraints from the void size function and of those from standard probes, like weak lensing, galaxy clustering and cluster counts (Contarini et al. 2022a; Pelliciari

et al. 2022). The expected gain is due to the strong complementarity between the confidence contours, appreciable in Figure 2. A brief explanation for the physical origin of this orthogonality is provided in Appendix C of Contarini et al. (2022b).

We now move to the analysis of the results for the  $\Omega_m$ - $H_0$  parameter plane. In Figure 3 we compare these constraints with selected noteworthy results from the literature. In the left panels of this figure, analogously to what we showed in Figure 2, we report the combination of the cosmological constraints from void counts with those derived from the analysis of void shape distortions (see Hamaus et al. 2020). The joint analysis of the two void statistics yields  $\Omega_m = 0.310^{+0.020}_{-0.021}$  and  $H_0 = 67.3^{+10.0}_{-9.1} \text{ km s}^{-1} \text{ Mpc}^{-1}$ .

In the right panels of Figure 3, we compare this result with the constraints obtained by Moresco et al. (2022) via the study of cosmic chronometers extracted from a combination of spectroscopic surveys, and the publicly available<sup>4</sup> results from the analysis of SN Ia, selected in the Pantheon+ sample (Scolnic et al. 2022; Brout et al. 2022a,b) including the cepheid host distances and covariance (SH0ES program, Riess et al. 2022). Albeit showing a large uncertainty with respect to standard probes, our result on  $H_0$  represents the very first estimate of the Hubble constant from cosmic voids — effectively opening the contribution of voids to the landscape of the  $H_0$  tension.

#### 4.2. The void perspective on cosmological tensions

In this section we firstly compute the value of  $S_8$  derived from the modeling of BOSS DR12 voids and

<sup>3</sup>This analysis concerns the modeling of three two-point functions: the cosmic shear correlation function, the galaxy angular auto-correlation and the galaxy-shear cross-correlation, and is commonly abbreviated as 3x2pt.

<sup>4</sup><https://github.com/PantheonPlusSH0ES/DataRelease>

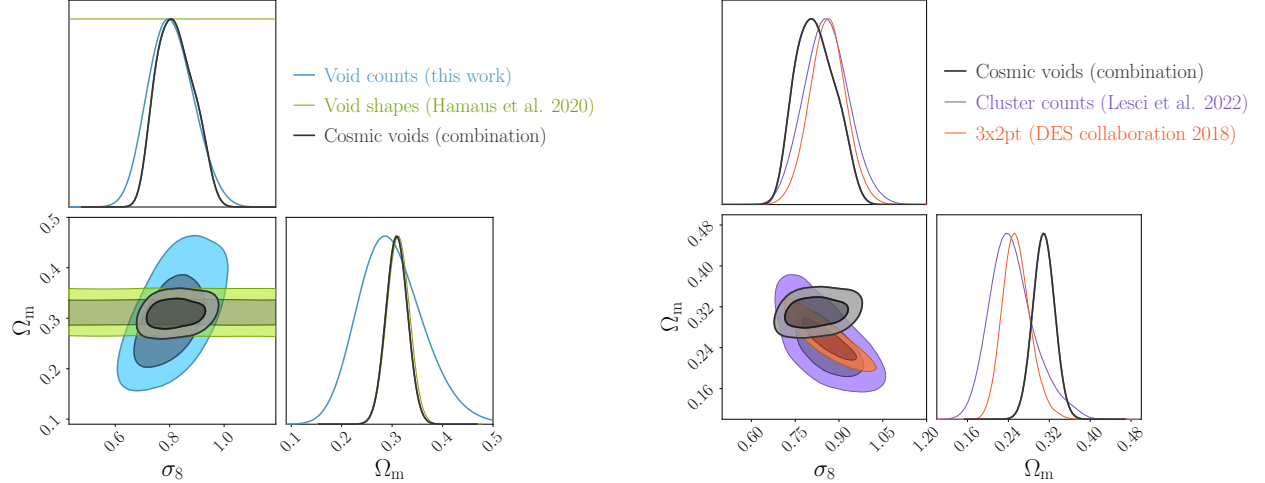


**Figure 2.** 68% and 95% confidence contours on the  $\Omega_m$ - $\sigma_8$  parameter plane and the corresponding projected posterior distributions. *Left:* confidence contours from void counts (light blue) and void shape distortions (green, from Hamaus et al. 2020) of BOSS DR12 voids, and their combination (black) as independent constraints. *Right:* comparison of the results from cosmic voids with other cosmological probes: cluster counts (purple, from Lesci et al. 2022) and the DES Y1 3x2pt analysis (red, from Dark Energy Survey Collaboration et al. 2018).

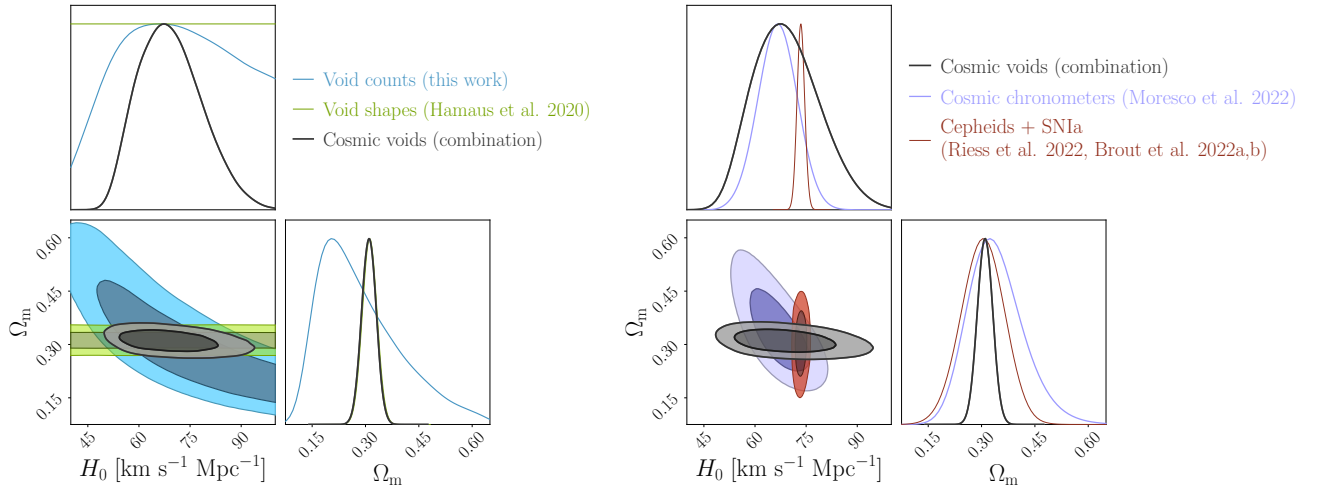


**Figure 3.** Same as Figure 2, but for the  $\Omega_m$ - $H_0$  parameter plane. In the right panel we now include constraints from cosmic chronometers in violet (Moresco et al. 2022) and from the distance ladder in dark red (Cepheids+SNIA, Riess et al. 2022; Brout et al. 2022a,b).

then compare it with selected results from the literature. From the analysis of void counts alone we derive a value of  $S_8 = 0.78^{+0.16}_{-0.15}$ , constrained with a precision of roughly 20%. This relatively large uncertainty is related to the definition of  $S_8$ : this derived parameter follows the main degeneracy direction of weak lensing and cluster counts measurements, which is unfavourable for perpendicular constraints, such as those obtained in our analysis. This behavior is naturally mitigated when including the contribution of void shape distortions, as shown in Section 4.1. In this case, we obtain a value of  $S_8 = 0.813^{+0.093}_{-0.068}$ , with an accuracy of 9.9%.

In Figure 4 we compare the latter result with the constraints derived in the following works (from top to bottom): Planck Collaboration et al. (2020) from CMB temperature and polarization, Semenaitė et al. (2022) from the full shape of anisotropic clustering measurements in BOSS and eBOSS, Lesci et al. (2022) from the mass function of clusters in KiDS DR3, the Dark Energy Survey Collaboration et al. (2018) from the 3x2pt analysis in DES Y1, Asgari et al. (2021) from cosmic shear in KiDS-1000, Philcox & Ivanov (2022) from the large-scale galaxy power spectrum and bispectrum monopole in the BOSS DR12, and Heymans et al. (2021) from the 3x2pt analysis in KiDS-1000. Although our constraints

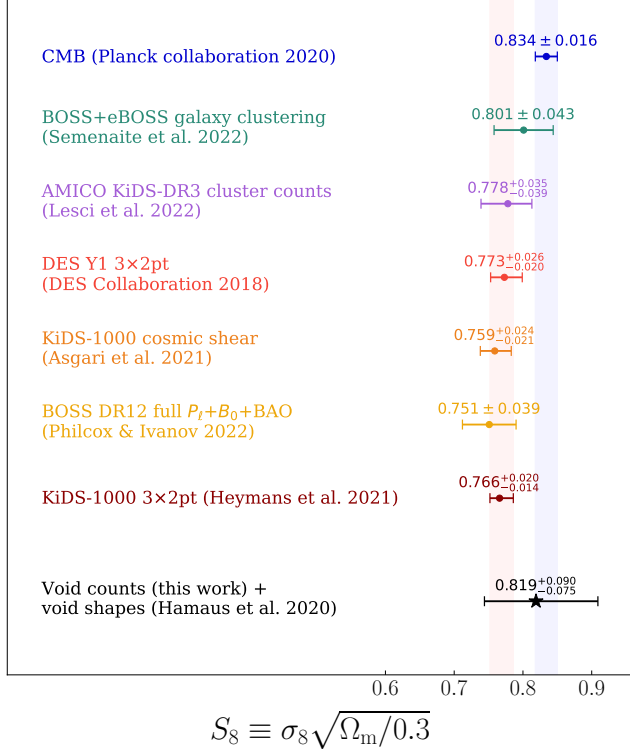


**Figure 4.** Comparison between recent constraints on the parameter  $S_8$  from different cosmological probes, with error bars representing the 68% confidence intervals. From top to bottom: Planck Collaboration et al. (2020), Semenaite et al. (2022), Lesci et al. (2022), Dark Energy Survey Collaboration et al. (2018), Asgari et al. (2021), Philcox & Ivanov (2022) and Heymans et al. (2021). The first and the last of these trace two reference bands, in blue and red respectively, highlighting the disagreement between the results at high and low redshift. We report our constraint on  $S_8$  at the bottom, with a black star with error bars.

cannot statistically exclude any of the  $S_8$  estimates reported, we note that the joint analysis of different void statistics provides cosmological constraints competitive with other methods in the literature, and is obtained with an independent methodology.

Moving on to the Hubble constant, we consider the constraint resulting from the joint analysis of void counts and shape distortions, since only the combination of these two void statistics allows us to break the degeneracy between  $\Omega_m$  and  $H_0$ . In Figure 5 we present a comparison of this result ( $H_0 = 67.3^{+10.0}_{-9.1} \text{ km s}^{-1} \text{ Mpc}^{-1}$ ) with recent selected cosmological constraints from the literature. From top to bottom we report the results by: the Planck Collaboration et al. (2020) from the analysis of CMB anisotropies, Moresco et al. (2022) from the study of cosmic chronometers, Semenaite et al. (2022) from the anisotropic clustering measurements in BOSS and eBOSS, The LIGO Scientific Collaboration et al.

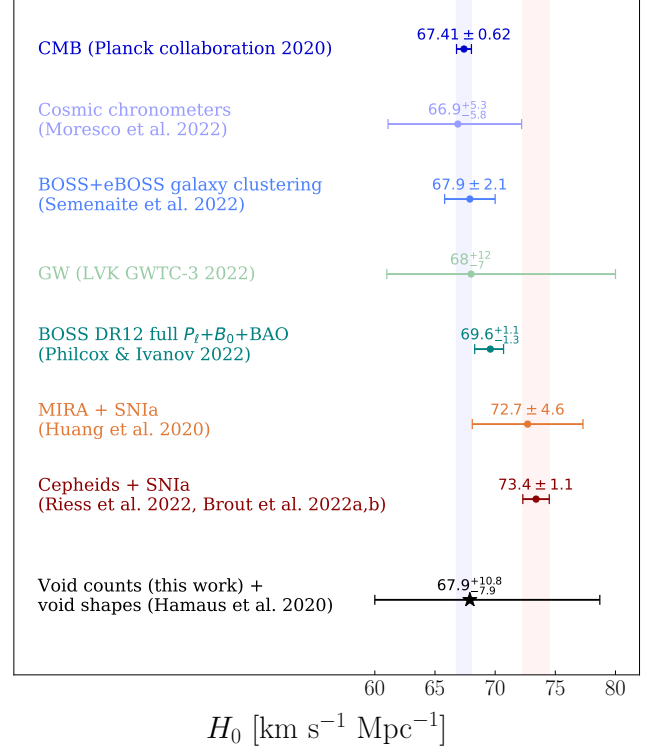


**Figure 5.** As Figure 4, but for the Hubble constant  $H_0$ . Here we compare our constraints (in black) with: Planck Collaboration et al. (2020), Moresco et al. (2022), Semenaite et al. (2022), The LIGO Scientific Collaboration et al. (2021), Philcox & Ivanov (2022), Huang et al. (2020) and Riess et al. (2022); Brout et al. (2022a,b).

(2021) using gravitational-wave sources extracted from the third LIGO-Virgo-KAGRA (LVK) Gravitational-Wave Transient Catalog (GWTC-3), Philcox & Ivanov (2022) from the full shape analysis of the power spectrum and bispectrum monopole of BOSS DR12 galaxies, Huang et al. (2020) exploiting the luminosity of a SN Ia calibrated with Hubble Space Telescope Mira variables, and finally Riess et al. (2022) and Brout et al. (2022a,b) from the analysis of Pantheon+ SN Ia calibrated with cepheids. This plot shows that our estimate of  $H_0$  from cosmic voids is fully consistent with all the presented cosmological constraints. We expect, however, to considerably improve the voids constraining power in the future, by extending the analysis to upcoming survey data and by including the contribution of other void statistics, e.g. void lensing and void clustering (Bonici et al. 2022; Kreisch et al. 2022).

## 5. Conclusions

In this *Letter*, we analyzed the size function of voids identified in the BOSS DR12 galaxies (Reid et al. 2016). We computed the void number counts in two redshift

bins and modeled them by means of an extension of the popular Vdn model (Jennings et al. 2013; Contarini et al. 2019, 2022b). The latter relies on two nuisance parameters,  $C_{\text{slope}}$  and  $C_{\text{offset}}$ , that we calibrated using 100 realizations of the official BOSS MultiDark PATCHY simulations (Kitaura et al. 2016). The modeling we considered consistently accounts for redshift-space and geometric distortions and was validated in Contarini et al. (2022b) on the PATCHY mocks. In a first attempt to exploit the combined power of different void statistics, we compute the constraints resulting from the combined analysis of void counts and shape distortions, the latter coming from Hamaus et al. (2020). The combination procedure we applied in this analysis assumed the two void statistics to be independent. Although potential cross-correlation matrix elements were not considered, their impact is expected to be negligible (Kreisch et al. 2022) and will be further explored in future studies.

We focused on the  $\Omega_m$ – $\sigma_8$  and  $\Omega_m$ – $H_0$  parameter planes, comparing our results with other selected noteworthy cosmological constraints from the literature, in the light of the modern cosmological tensions. First, we presented the results derived from the combination of the two selected void statistics, investigating the  $S_8 \equiv \sigma_8 \sqrt{\Omega_m / 0.3}$  tension. obtained the marginalized constraints  $\Omega_m = 0.308^{+0.021}_{-0.018}$  and  $\sigma_8 = 0.809^{+0.072}_{-0.068}$ , which translate into the derived parameter  $S_8 = 0.813^{+0.093}_{-0.068}$ . These results are both competitive and compatible with cosmological constraints derived from other probes, such as the void-galaxy cross-correlation function, galaxy cluster number counts, the 3x2pt statistics and others.

We then oriented our analysis towards the  $H_0$  tension, deriving from the analysis of different void statistics the marginalized constraints  $\Omega_m = 0.310^{+0.020}_{-0.021}$  and  $H_0 = 67.3^{+10.0}_{-9.1} \text{ km s}^{-1} \text{ Mpc}^{-1}$ . Due to the large uncertainty on the estimate of  $H_0$ , our constraints are in agreement with various results from the literature, such as those derived from the analysis of CMB anisotropies in the Planck Collaboration et al. (2020) and from SN Ia by Riess et al. (2022) and Brout et al. (2022a,b).

At this stage, the presented constraints on the  $S_8$  and  $H_0$  parameters do not allow us to take a decisive position in the context of the current cosmological tensions. Nevertheless, this work shows for the first time the relevance of cosmic voids in the context of modern tensions in cosmology, providing an independent probe. We plan to extend our analysis to the data of upcoming wide-field surveys like *Euclid* (Laureijs et al. 2011; Amendola et al. 2018), the Dark Energy Spectroscopic Instrument (DESI Collaboration et al. 2016), the Nancy Grace Ro-

man Space Telescope (NGRST, Spergel et al. 2015), and the Vera C. Rubin Observatory (Ivezic et al. 2019).

SC thanks Michele Moresco, Alfonso Veropalumbo, Giorgio Lesci and Nicola Borghi for the contribution and suggestions they provided. AP is grateful to Scott Dodelson for useful discussions. The authors thank Steffen Hagstotz, Barbara Sartoris, Nico Schuster, Giovanni Verza and Ben Wandelt for useful conversations. We acknowledge the grant ASI n.2018-23-HH.0. SC, FM, LM and MB acknowledge the use of computational resources from the parallel computing cluster of the Open Physics Hub (<https://site.unibo.it/openphysicshub/en>) at the Physics and Astronomy Department in Bologna. AP is supported by NASA ROSES grant 12-EUCLID12-0004, and NASA grant 15-WFIRST15-0008 to the Nancy Grace Roman Space Telescope Science Investigation Team “Cosmology with the High Latitude Survey”. AP acknowledges support from the Simons Foundation to the Center for Computational Astrophysics at the Flatiron Institute. NH is supported by the Excellence Cluster ORIGINS, which is funded by the Deutsche Forschungsgemeinschaft (DFG, German Research Foundation) under Germany’s Excellence Strategy – EXC-2094 – 390783311. LM acknowledges support from PRIN MIUR 2017 WSCC32 “Zooming into dark matter and proto-galaxies with massive lensing clusters”. We acknowledge use of the Python libraries NumPy (Harris et al. 2020), Matplotlib (Hunter 2007) and ChainConsumer (Hinton 2016).

## References

Abdalla, E., Abellán, G. F., Aboubrahim, A., et al. 2022, Journal of High Energy Astrophysics, 34, 49, doi: [10.1016/j.jheap.2022.04.002](https://doi.org/10.1016/j.jheap.2022.04.002)

Alcock, C., & Paczynski, B. 1979, Nature, 281, 358, doi: [10.1038/281358a0](https://doi.org/10.1038/281358a0)

Amendola, L., Appleby, S., Avgoustidis, A., et al. 2018, Living Reviews in Relativity, 21, 2, doi: [10.1007/s41114-017-0010-3](https://doi.org/10.1007/s41114-017-0010-3)

Asgari, M., Lin, C.-A., Joachimi, B., et al. 2021, A&A, 645, A104, doi: [10.1051/0004-6361/202039070](https://doi.org/10.1051/0004-6361/202039070)

Aubert, M., Cousinou, M.-C., Escoffier, S., et al. 2022, MNRAS, 513, 186, doi: [10.1093/mnras/stac828](https://doi.org/10.1093/mnras/stac828)

Bayer, A. E., Liu, J., Terasawa, R., et al. 2022, arXiv e-prints, arXiv:2210.15647. <https://arxiv.org/abs/2210.15647>

Bonici, M., Carbone, C., Vielzeuf, P., et al. 2022, arXiv e-prints, arXiv:2206.14211. <https://arxiv.org/abs/2206.14211>

Brout, D., Taylor, G., Scolnic, D., et al. 2022a, ApJ, 938, 111, doi: [10.3847/1538-4357/ac8bcc](https://doi.org/10.3847/1538-4357/ac8bcc)

Brout, D., Scolnic, D., Popovic, B., et al. 2022b, ApJ, 938, 110, doi: [10.3847/1538-4357/ac8e04](https://doi.org/10.3847/1538-4357/ac8e04)

Contarini, S., Verza, G., Pisani, A., et al. 2022a, *A&A*, 667, A162, doi: [10.1051/0004-6361/202244095](https://doi.org/10.1051/0004-6361/202244095)

Contarini, S., Marulli, F., Moscardini, L., et al. 2021, *MNRAS*, 504, 5021, doi: [10.1093/mnras/stab1112](https://doi.org/10.1093/mnras/stab1112)

Contarini, S., Pisani, A., Hamaus, N., et al. 2022b, arXiv e-prints, arXiv:2212.03873. <https://arxiv.org/abs/2212.03873>

Contarini, S., Ronconi, T., Marulli, F., et al. 2019, *MNRAS*, 488, 3526, doi: [10.1093/mnras/stz1989](https://doi.org/10.1093/mnras/stz1989)

Dark Energy Survey Collaboration, Abbott, T. M. C., Abdalla, F. B., et al. 2018, *PhRvD*, 98, 043526, doi: [10.1103/PhysRevD.98.043526](https://doi.org/10.1103/PhysRevD.98.043526)

Dawson, K. S., Schlegel, D. J., Ahn, C. P., et al. 2013, *AJ*, 145, 10, doi: [10.1088/0004-6256/145/1/10](https://doi.org/10.1088/0004-6256/145/1/10)

DESI Collaboration, Aghamousa, A., Aguilar, J., et al. 2016, arXiv:1611.00036. <https://arxiv.org/abs/1611.00036>

Di Valentino, E., Anchordoqui, L. A., Akarsu, Ö., et al. 2021a, *Astroparticle Physics*, 131, 102605, doi: [10.1016/j.astropartphys.2021.102605](https://doi.org/10.1016/j.astropartphys.2021.102605)

—. 2021b, *Astroparticle Physics*, 131, 102604, doi: [10.1016/j.astropartphys.2021.102604](https://doi.org/10.1016/j.astropartphys.2021.102604)

Di Valentino, E., Mena, O., Pan, S., et al. 2021c, *Classical and Quantum Gravity*, 38, 153001, doi: [10.1088/1361-6382/ac086d](https://doi.org/10.1088/1361-6382/ac086d)

Eisenstein, D. J., Weinberg, D. H., Agol, E., et al. 2011, *AJ*, 142, 72, doi: [10.1088/0004-6256/142/3/72](https://doi.org/10.1088/0004-6256/142/3/72)

Hamaus, N., Aubert, M., Pisani, A., et al. 2022, *A&A*, 658, A20, doi: [10.1051/0004-6361/202142073](https://doi.org/10.1051/0004-6361/202142073)

Hamaus, N., Pisani, A., Choi, J.-A., et al. 2020, *JCAP*, 2020, 023, doi: [10.1088/1475-7516/2020/12/023](https://doi.org/10.1088/1475-7516/2020/12/023)

Hamaus, N., Pisani, A., Sutter, P. M., et al. 2016, *PhRvL*, 117, 091302, doi: [10.1103/PhysRevLett.117.091302](https://doi.org/10.1103/PhysRevLett.117.091302)

Harris, C. R., Millman, K. J., van der Walt, S. J., et al. 2020, *Nature*, 585, 357, doi: [10.1038/s41586-020-2649-2](https://doi.org/10.1038/s41586-020-2649-2)

Heymans, C., Tröster, T., Asgari, M., et al. 2021, *A&A*, 646, A140, doi: [10.1051/0004-6361/202039063](https://doi.org/10.1051/0004-6361/202039063)

Hinton, S. R. 2016, *The Journal of Open Source Software*, 1, 00045, doi: [10.21105/joss.00045](https://doi.org/10.21105/joss.00045)

Huang, C. D., Riess, A. G., Yuan, W., et al. 2020, *ApJ*, 889, 5, doi: [10.3847/1538-4357/ab5dbd](https://doi.org/10.3847/1538-4357/ab5dbd)

Hunter, J. D. 2007, *Computing in Science & Engineering*, 9, 90, doi: [10.1109/MCSE.2007.55](https://doi.org/10.1109/MCSE.2007.55)

Ivezić, Ž., Kahn, S. M., Tyson, J. A., et al. 2019, *ApJ*, 873, 111, doi: [10.3847/1538-4357/ab042c](https://doi.org/10.3847/1538-4357/ab042c)

Jennings, E., Li, Y., & Hu, W. 2013, *MNRAS*, 434, 2167, doi: [10.1093/mnras/stt1169](https://doi.org/10.1093/mnras/stt1169)

Kitaura, F.-S., Rodríguez-Torres, S., Chuang, C.-H., et al. 2016, *MNRAS*, 456, 4156, doi: [10.1093/mnras/stv2826](https://doi.org/10.1093/mnras/stv2826)

Kitaura, F. S., Yepes, G., & Prada, F. 2014, *MNRAS*, 439, L21, doi: [10.1093/mnrasl/slt172](https://doi.org/10.1093/mnrasl/slt172)

Klypin, A., Yepes, G., Gottlöber, S., Prada, F., & Heß, S. 2016, *MNRAS*, 457, 4340, doi: [10.1093/mnras/stw248](https://doi.org/10.1093/mnras/stw248)

Kovács, A., Vielzeuf, P., Ferrero, I., et al. 2022, *MNRAS*, 515, 4417, doi: [10.1093/mnras/stac2011](https://doi.org/10.1093/mnras/stac2011)

Kreisch, C. D., Pisani, A., Villaescusa-Navarro, F., et al. 2022, *ApJ*, 935, 100, doi: [10.3847/1538-4357/ac7d4b](https://doi.org/10.3847/1538-4357/ac7d4b)

Laureijs, R., Amiaux, J., Arduini, S., et al. 2011, ArXiv e-prints. <https://arxiv.org/abs/1110.3193>

Lesci, G. F., Marulli, F., Moscardini, L., et al. 2022, *A&A*, 659, A88, doi: [10.1051/0004-6361/202040194](https://doi.org/10.1051/0004-6361/202040194)

Marulli, F., Veropalumbo, A., & Moresco, M. 2016, *Astronomy and Computing*, 14, 35, doi: [10.1016/j.ascom.2016.01.005](https://doi.org/10.1016/j.ascom.2016.01.005)

Moresco, M., Amati, L., Amendola, L., et al. 2022, arXiv:2201.07241. <https://arxiv.org/abs/2201.07241>

Nadathur, S., Woodfinden, A., Percival, W. J., et al. 2020, *MNRAS*, 499, 4140, doi: [10.1093/mnras/staa3074](https://doi.org/10.1093/mnras/staa3074)

Neyrinck, M. C. 2008, *MNRAS*, 386, 2101, doi: [10.1111/j.1365-2966.2008.13180.x](https://doi.org/10.1111/j.1365-2966.2008.13180.x)

Pandey, K. L., Karwal, T., & Das, S. 2020, *JCAP*, 2020, 026, doi: [10.1088/1475-7516/2020/07/026](https://doi.org/10.1088/1475-7516/2020/07/026)

Pelliciari, D., Contarini, S., Marulli, F., et al. 2022, arXiv e-prints, arXiv:2210.07248. <https://arxiv.org/abs/2210.07248>

Philcox, O. H. E., & Ivanov, M. M. 2022, *PhRvD*, 105, 043517, doi: [10.1103/PhysRevD.105.043517](https://doi.org/10.1103/PhysRevD.105.043517)

Pisani, A., Massara, E., Spergel, D. N., et al. 2019, *BAAS*, 51, 40. <https://arxiv.org/abs/1903.05161>

Planck Collaboration, Ade, P. A. R., Aghanim, N., et al. 2014, *A&A*, 571, A16, doi: [10.1051/0004-6361/201321591](https://doi.org/10.1051/0004-6361/201321591)

Planck Collaboration, Aghanim, N., Akrami, Y., et al. 2020, *A&A*, 641, A1, doi: [10.1051/0004-6361/201833880](https://doi.org/10.1051/0004-6361/201833880)

Platen, E., van de Weygaert, R., & Jones, B. J. T. 2007, *MNRAS*, 380, 551, doi: [10.1111/j.1365-2966.2007.12125.x](https://doi.org/10.1111/j.1365-2966.2007.12125.x)

Reid, B., Ho, S., Padmanabhan, N., et al. 2016, *MNRAS*, 455, 1553, doi: [10.1093/mnras/stv2382](https://doi.org/10.1093/mnras/stv2382)

Riess, A. G., Yuan, W., Macri, L. M., et al. 2022, *ApJL*, 934, L7, doi: [10.3847/2041-8213/ac5c5b](https://doi.org/10.3847/2041-8213/ac5c5b)

Rodríguez-Torres, S. A., Chuang, C.-H., Prada, F., et al. 2016, *MNRAS*, 460, 1173, doi: [10.1093/mnras/stw1014](https://doi.org/10.1093/mnras/stw1014)

Ronconi, T., Contarini, S., Marulli, F., Baldi, M., & Moscardini, L. 2019, *MNRAS*, 488, 5075, doi: [10.1093/mnras/stz2115](https://doi.org/10.1093/mnras/stz2115)

Ronconi, T., & Marulli, F. 2017, *A&A*, 607, A24, doi: [10.1051/0004-6361/201730852](https://doi.org/10.1051/0004-6361/201730852)

Sahlén, M., Zubeldía, I., & Silk, J. 2016, *ApJL*, 820, L7, doi: [10.3847/2041-8205/820/1/L7](https://doi.org/10.3847/2041-8205/820/1/L7)

Sánchez, A. G., Scoccimarro, R., Crocce, M., et al. 2017, *MNRAS*, 464, 1640, doi: [10.1093/mnras/stw2443](https://doi.org/10.1093/mnras/stw2443)

Schöneberg, N., Abellán, G. F., Sánchez, A. P., et al. 2022, *PhR*, 984, 1, doi: [10.1016/j.physrep.2022.07.001](https://doi.org/10.1016/j.physrep.2022.07.001)

Scolnic, D., Brout, D., Carr, A., et al. 2022, *ApJ*, 938, 113, doi: [10.3847/1538-4357/ac8b7a](https://doi.org/10.3847/1538-4357/ac8b7a)

Semenaitė, A., Sánchez, A. G., Pezzotta, A., et al. 2022, *MNRAS*, 512, 5657, doi: [10.1093/mnras/stac829](https://doi.org/10.1093/mnras/stac829)

Sheth, R. K., & van de Weygaert, R. 2004, *MNRAS*, 350, 517, doi: [10.1111/j.1365-2966.2004.07661.x](https://doi.org/10.1111/j.1365-2966.2004.07661.x)

Spergel, D., Gehrels, N., Baltay, C., et al. 2015, arXiv:1503.03757. <https://arxiv.org/abs/1503.03757>

Sutter, P. M., Lavaux, G., Hamaus, N., et al. 2015, *Astronomy and Computing*, 9, 1, doi: [10.1016/j.ascom.2014.10.002](https://doi.org/10.1016/j.ascom.2014.10.002)

Taruya, A., Nishimichi, T., & Saito, S. 2010, *PhRvD*, 82, 063522, doi: [10.1103/PhysRevD.82.063522](https://doi.org/10.1103/PhysRevD.82.063522)

The LIGO Scientific Collaboration, the Virgo Collaboration, the KAGRA Collaboration, et al. 2021, arXiv e-prints, arXiv:2111.03604. <https://arxiv.org/abs/2111.03604>

Verza, G., Pisani, A., Carbone, C., Hamaus, N., & Guzzo, L. 2019, *JCAP*, 2019, 040, doi: [10.1088/1475-7516/2019/12/040](https://doi.org/10.1088/1475-7516/2019/12/040)

Woodfinden, A., Nadathur, S., Percival, W. J., et al. 2022, *MNRAS*, 516, 4307, doi: [10.1093/mnras/stac2475](https://doi.org/10.1093/mnras/stac2475)